

ON THE HOMOGENEITY OF TURBULENCE GENERATED BY STATIC GRIDS

Özgür ErtuncInstitute of Fluid Mechanics (LSTM-Erlangen)
Friedrich-Alexander-Universität Erlangen-Nürnberg,
Cauerstr.4 D-91058 Erlangen, Germany
ertunc@lstm.uni-erlangen.de**Hermann Lienhart**Institute of Fluid Mechanics (LSTM-Erlangen)
Friedrich-Alexander-Universität Erlangen-Nürnberg,
Cauerstr.4 D-91058 Erlangen, Germany
lienhart@lstm.uni-erlangen.de**Franz Durst**FMP Technology GmbH,
Am Weichselgarten 34 D-91058 Erlangen, Germany
f.durst@fmp-technology.com**ABSTRACT**

The homogeneities of unstrained and strained turbulence, which was generated by static grids, were investigated with the help of hot-wire measurements. Two different facilities, one closed loop and one open loop wind tunnel were employed for the investigations. It is shown that the mean streamwise velocity becomes rapidly homogeneous downstream of the grids which had porosities of 64% and 67%. In contrast to the mean streamwise velocity, Reynolds stresses and their anisotropy stay inhomogeneous for a long stretch downstream of the grid, although the porosities of the grids were higher than the lowest 57% suggested in the literature as the lowest porosity to realize homogeneous turbulence downstream of a grid. Furthermore, independent of the mesh Reynolds number, inhomogeneities of the turbulence quantities persist at the same spatial locations. When grid-generated turbulence is exposed to positive axisymmetric strain through a nozzle, it was observed that the inhomogeneous regions disappear just after turbulence becomes isotropic. The constants in the power decay laws of turbulence quantities were evaluated in the inhomogeneous grid-generated turbulence field and in the turbulence field homogenized by a nozzle with a slight contraction. It is demonstrated that constants of decay laws scatter more in the inhomogeneous field than in the homogeneous field.

INTRODUCTION

Homogeneous turbulent flows have been the subject of numerous investigations of turbulence due to their statistical properties, among which the invariance of all statistical moments to translation is the most important. Owing to the translational invariance of homogeneous turbulence, decay processes in undistorted flows and the effects of mean velocity distortion on this kind of turbulent flows have constituted the framework of understanding and modelling of turbulent flow phenomena (for a review, see Gence, 1983).

In experimental investigations, homogeneous turbulence has commonly been produced by static grid structures. Although the generated turbulence is not spatially homoge-

neous in the flow direction owing to its decay or the influence of mean velocity distortion on turbulence, these changes are treated as changes in time for a Lagrangian fluid element using Taylor's frozen turbulence assumption. Hence, throughout this paper we treat homogeneity of turbulence in the planes perpendicular to the flow direction. In order to ensure the homogeneity of the turbulent flow field in the wake of a grid, Corrsin (1963) suggested that three conditions should be satisfied. First, the grid should have a porosity larger than 57% to prevent coalescing jets. Second, the diameter or the height of the flow duct, say D , must be much larger than the length scale of the energy-containing eddies which is of the same order as the mesh size of the grid (M), i.e. $D/M \gg 1$. Since the boundary layer scales with the mesh size, the larger the ratio D/M the less any effect of the walls on the measured data is expected. Third, the measurements should be taken far downstream, since the turbulence becomes homogeneous only after at least 40 mesh sizes downstream of the grid. A lack of one or more of these conditions might lead to inhomogeneity and, therefore, the resultant data must not be compared with the laws deduced for homogeneous turbulence. In other words, after fulfilling these conditions, measurements of undistorted and distorted grid-generated turbulence were expected to reflect the properties of homogeneous turbulence.

Most of the studies on homogeneous turbulence have satisfied these conditions. However, to the best of the authors' knowledge, there are only a few studies in the literature which directly investigated the homogeneity of the grid-generated turbulence. Batchelor and Townsend (1948) and Batchelor and Stewart (1950) recognized the lack of homogeneity for very fine grids (grids of 1/4 inch mesh size). Grant and Nisbet (1957) showed that the inhomogeneity of Reynolds stresses can reach up to $\pm 15\%$ at $x_1/M = 80$ for a mesh size of 1/4 inch and $\pm 6\%$ at $x_1/M = 30$ for a 2 inch mesh size. Additionally, their transverse profile measurements in the wake of the grids showed wavy r.m.s. values of turbulent velocity fluctuations. All their grids had a porosity of 70%, i.e. much larger than the value suggested by Corrsin. Their investigations revealed that, with increasing mesh size,

the inhomogeneity dropped. Moreover, they showed that the location of the measurement axis along the flow direction has a drastic effect on the constants of the decay law of grid-generated turbulence. In a detailed study on turbulence manipulators, Loehrke and Nagib (1972) observed also standing wavy structures in the wake of the grids and honeycombs. In a later study by Liu et al. (2004), the inhomogeneity of the r.m.s. of velocity fluctuations increased in the streamwise direction, reaching up to 30% at $x_1/M = 40$ for perforated plates of 65% porosity. They showed that the higher the solidity, the higher is the inhomogeneity of turbulence and, for a constant porosity, the higher the mesh diameter the lower is the inhomogeneity of the r.m.s. of velocity fluctuations. The literature shows that although grid-generated turbulence was utilized in many experimental turbulence investigations, its homogeneity did not receive proper attention and, consequently, was mostly accepted as an ad hoc assumption.

During our studies on homogeneous turbulence, it was found essential to determine the extent of spatial homogeneity of grid-generated turbulence. Detailed hot-wire measurements (Ertunç and Lienhart, 2006; Ertunç, 2007) were conducted in the wake of grids with 64% and 67% porosity, which were higher than the 57% porosity suggested by Corrsin (1963). These measurements revealed inhomogeneous Reynolds stress fields far downstream of the grid ($x_1/M > 40$) and an homogenization effect of positive axisymmetric strain. Therefore, we found it necessary to readdress the problem of spatial homogeneity of turbulence generated by static grid structures and summarize the results of our experimental investigations. The main objectives of the investigations presented here were to determine the extent of homogeneity of mean velocity and Reynolds stress fields, the dependence of homogeneity on the mesh Reynolds number and the influence of positive axisymmetric strain (flow through an axisymmetric contraction) on the spatial homogeneity of turbulence.

FLOW FACILITIES AND INSTRUMENTATION

For the measurements of turbulent velocity fluctuations downstream of a static grid structure, two wind tunnels of LSTM-Erlangen were employed. The effect of the mesh Reynolds number on the homogeneity of grid-generated turbulence was investigated in the closed-loop wind tunnel of LSTM-Erlangen (Fig. 1a) and the effect of positive axisymmetric strain was investigated in the axisymmetric strain wind tunnel of LSTM-Erlangen (AST) (Fig. 2).

The test section of the wind tunnel was almost completely closed to prevent the generation of free shear turbulence at the edges of the flow in the test section and its influence on the measurements. The closed part of the test section was 1.87 m in width, 1.40 m in height and 2.0 m in length. In Fig. 1 b, the test section, the static grid structure and the hot-wire probe measurement equipment employed in these investigations are shown. As can be seen in the photograph, the hot-wire probes were mounted on a 3-D traversing system. A square punched grid structure with a 10 mm mesh size, M , with 64% porosity was installed at the exit of the contraction. In accordance with the above-mentioned studies, the mesh size is defined as the distance from the center of one rod to the next. The ratio between any one of the cross-sectional dimensions of the test section and the mesh size was much larger than 1. The selected mesh size allowed measurements to be conducted at distances more than $100M$ downstream of the grid in this test section. The

mesh Reynolds number,

$$Re_M = \frac{U_m M}{\nu}, \quad (1)$$

was controlled by setting the mean flow speed in the test section, U_m . In this way, the effects of mesh Reynolds number on the inhomogeneity of measured turbulence quantities could be checked. The wind tunnel was equipped with a temperature control, which kept the flow at a given temperature within ± 0.5 K. The maximum operating speed in the test section could be set up to 60 m/s. Because of the large drag force applied on the grid at high velocities and the resulting deformation of the grid, in the present investigations only velocities up to 12 m/s were considered.

The AST and the measurement instruments are sketched in Fig. 2. The main components of this experimental facility were an open-circuit sucking-type wind tunnel driven downstream by a radial blower (14). For the investigations presented here, turbulence was generated by a square punched metal grid (5) with 67% porosity and 12 mm mesh size. In order to generate positive axisymmetric strain in the AST, two different axisymmetric contracting nozzles (8) were employed with contraction ratios of 1.27 and 3.69, respectively, downstream of the grid structure. The contraction ratio is defined as the ratio between the inlet and the outlet area of the nozzle, $c = A_{inlet}/A_{outlet}$. For hot-wire measurements at various locations in the flow, the hot-wire probes (7) were mounted on a traversing unit (9), enabling movements in all three orthogonal directions. To permit undisturbed measurements, the test section and the traversing unit were located inside an acoustically damped chamber (19). A detailed description of the AST can be found in Ertunç (2007).

In both flow facilities, almost identical instruments, which are shown in Fig. 2, were used for the measurements. To conduct velocity measurements, a DISA 56C01 hot-wire anemometer unit with four DISA CT56C17 constant-temperature hot-wire bridges was employed. Two single normal wire (SN-wire) and one X-wire probe were used. This probe configuration was selected to account for the irrotational velocity fluctuations appearing as flow disturbances. The theoretical background of the design of this probe system and the necessary measurement and data processing methods were given in detail by Ertunç (2007) and Ertunç and Durst (2008).

The normal wires were 0.8 and 1.0 mm in length and the two inclined wires of the X-wire probe were 1.2 mm in length. The distance between the inclined wires of the X-wire probe was 1.0 mm and their geometric inclinations were 43° and 44° with respect to the probe axis. All the hot-wires employed were $5 \mu\text{m}$ in diameter. The settings of the hot-wire bridges, the data acquisition system and the selected number of independent samples permitted low-turbulence intensity measurements, with high digitalization and statistical accuracy. For the Reynolds stresses, the statistical error was estimated to be less than $\pm 1.2\%$ (for more details, see Ertunç, 2007).

Overview of Experiments

The hot-wire measurements in the wind tunnel comprised scans in a plane, which was perpendicular to the grid, located about the center of the test section and extending 1060 mm in the streamwise direction and 50 mm in the transverse direction. The transverse and streamwise resolutions of the scan were 1 mm and 10 mm, respectively. Since such a measurement field corresponds to a long narrow stripe, the

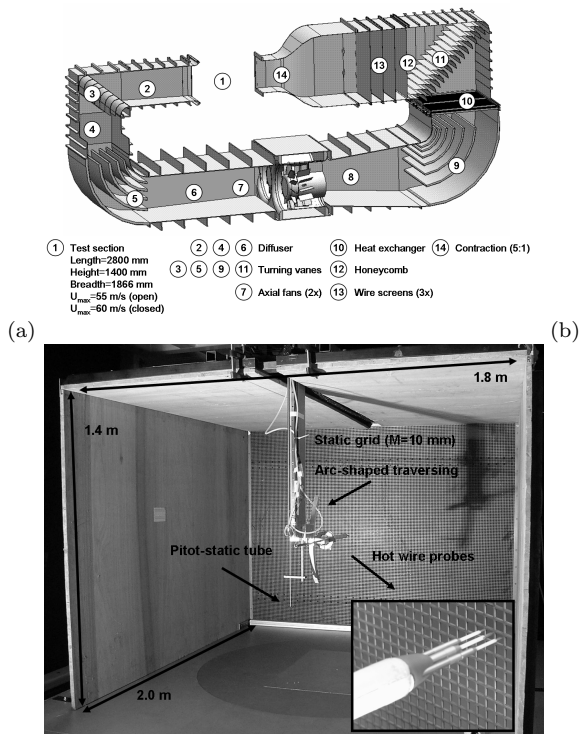


Figure 1: (a) The closed-loop wind tunnel of LSTM-Erlangen; (b) the test section of the wind tunnel and the installed measurement system.

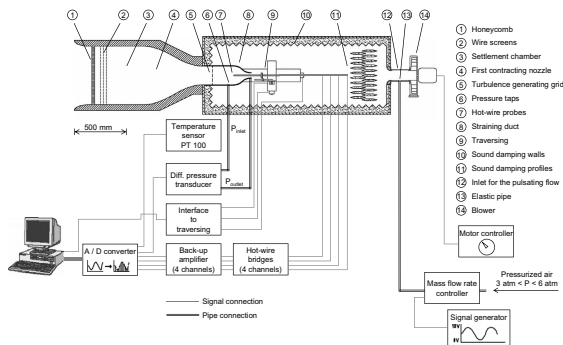


Figure 2: The axisymmetric strain wind tunnel (AST) of LSTM-Erlangen and the instrumentation.

Table 1: Overview of test cases reported in this paper.

c	Re_M	Porosity
1	4000, 5333, 8000	64 %
1.27	4066	67 %
3.69	4066	67 %

measured field could only be visualized by reducing the aspect ratio in the plots. The widths of the scanned planes in the AST was also 50 mm, but their length varied depending on the test case. The experiments with the $c = 3.69$ nozzle extended from the vicinity of the grid to the exit of the nozzle, whereas experiments with $c = 1.27$ were conducted downstream of the nozzle within a duct with constant diameter. An overview of the experiments is given in Table 1.

Analyzed Quantities

The scanned planes consist of N_{x_1} points in the flow direction and N_{x_2} points in the transverse direction, such that the spatial resolutions of the scan in both directions are Δx_1 and Δx_2 . In order to visualize the homogeneity of any one of the measured mean quantities, say \bar{H} , in the scanned plane, the inhomogeneity parameter $I_{\bar{H}}$ is defined as:

$$I_{\bar{H}}(x_1, x_2) = \frac{\bar{H}(i\Delta x_1, j\Delta x_2)}{\left| \frac{1}{N_{x_2}} \sum_{j=1}^{N_{x_2}} \bar{H}(i\Delta x_1, j\Delta x_2) \right|} 100, \quad (2)$$

which is the percentage deviation of the variable $\bar{H}(x_1, x_2)$ from the absolute value of its average value calculated along a line $x_1 = \text{constant}$. The inhomogeneity of the mean longitudinal velocity $I_{\bar{U}_1}$ and the Reynolds stresses, e.g. $I_{\overline{u_1 u_1}}$, are analyzed in the following. Anisotropies of Reynolds stresses, which are non-dimensional parameters, are of vital importance for modeling and predictions. Therefore, the field of stress anisotropy and its inhomogeneity is visualized by using the anisotropy of longitudinal normal Reynolds stress a_{11} , which is

$$a_{11} = \frac{\overline{u_1 u_1}}{q^2} - \frac{1}{3}, \quad (3)$$

where $q^2 = \overline{u_1 u_1} + \overline{u_2 u_2} + \overline{u_3 u_3}$ and can be approximated by $q^2 \approx \overline{u_1 u_1} + 2\overline{u_2 u_2}$ in the nearly homogeneous and axisymmetric turbulence, which was expected to be the case for grid-generated turbulence.

Moreover, in an ideal homogeneous turbulence, distribution functions of velocity fluctuations, for instance streamwise (u_1) and transverse (u_2) velocity fluctuations, should show a symmetry around their zero mean and should have a normal distribution. The symmetry of u_1 fluctuations is monitored through the skewness factor:

$$S_{u_1} = \frac{\overline{u_1^3}}{\sqrt{\overline{u_1 u_1}}^3}. \quad (4)$$

For a perfect symmetric distribution, the skewness factor should be zero. The flatness factor for u_1 fluctuations:

$$F_{u_1} = \frac{\overline{u_1^4}}{\sqrt{\overline{u_1 u_1}}^4} \quad (5)$$

is a measure of the normal distribution and it should be 3 for a perfect normal distribution.

EXPERIMENTAL RESULTS

Unstrained Turbulence

The inhomogeneity of the mean velocity field at $Re_M = 8000$ is shown in Fig. 3. The locations of grid rods are depicted as black bars on the vertical axis. It is obvious that mean velocity ceases behind the rods and increases in the open area between two rods. In the vicinity of the grid $x_1/M < 10$, $I_{\bar{U}_1}$ is over $\pm 10\%$ but it decreases below $\pm 2\%$ for $x_1/M > 15$ and levels to $\pm 1\%$ for $x_1/M > 50$.

The inhomogeneity of the normal stress $\overline{u_1 u_1}$ for different flow speeds, i.e. $Re_M = 4000, 5333$ and 8000 , are shown in Fig. 4. Broadly seen are the regions having either positive or negative deviations extending in the whole streamwise direction. In the $I_{\overline{u_1 u_1}}$ field (also in the inhomogeneity fields of other Reynolds stress components, which are not shown here), traces of each grid rod can clearly be seen up to $x_1/M \approx 12$. Further downstream of the grid at $x_1/M > 10$ positive regions coalesce with positive regions and vice versa so that wider stripes of positive and

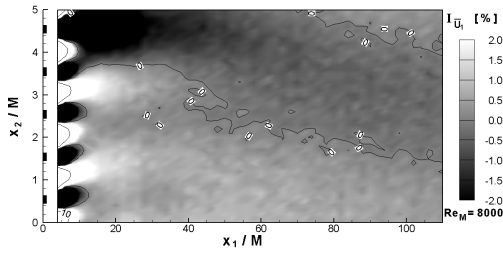


Figure 3: Inhomogeneity of the mean velocity field $I_{\bar{u}_1}$ at the wake of the grid in the wind tunnel at $Re_M = 8000$.

negative regions occur which again coalesce with each other. In three dimensions the inhomogeneity field can be imagined to be composed of continuously braiding positive and negative stripes. In the wake of the grid, the levels of inhomogeneities of the normal stresses do not drop but spatially fluctuate between $\pm 5\%$. These regions are repeating in a cyclic manner in the transverse direction, but not with a period of mesh size M . It can be concluded that measurements of normal stresses along any two lines with $x_2 = \text{constant}$ might deviate $\pm 5\%$ from each other. The inhomogeneity of the other Reynolds stresses, $\overline{u_2 u_2}$ and $\overline{u_1 u_2}$, also revealed similar inhomogeneous fields (Ertunç and Lienhart, 2006; Ertunç, 2007). It is useful to note that the total measuring time of one of these planes for one Re_M was around 3 days. Hence, it is really impressive to observe the spatially stable inhomogeneity fields behind the grid even after 100 mesh sizes and the persistence of these regions in time for all Reynolds numbers. In order to check the influence of tolerances in the grid geometry, Ertunç et al. (2008) conducted direct numerical simulations and could show that even the perfectly uniform grid structure generates an inhomogeneous turbulence field in its wake.

The anisotropy a_{11} field and its inhomogeneity $I_{a_{11}}$ field are shown in Fig. 5. In the flow direction a_{11} has a tendency to drop (Fig. 5a). However, a_{11} decreases faster close to the grid and further downstream it levels to some value, which is dependent on the grid Reynolds number and the measurement location (Ertunç, 2007). The negative and positive stripes of inhomogeneity can also be seen in Fig. 5 b with deviations approaching $\pm 20\%$ far downstream of the grid.

The skewness and flatness factors of u_1 fluctuations and, particularly, u_2 fluctuations also show spatially inhomogeneous fields. Examples of those fields of u_2 fluctuations are presented in Fig. 6 for $Re_M = 8000$. For $x_1/M > 12$, the skewness factors take values ± 0.1 . In the detailed analysis of the measured data, Ertunç (2007) showed that the spatial inhomogeneity of F_{u_2} close to the grid grows with the increasing Reynolds number. Further downstream of the grid, both flatness factors, F_{u_1} and F_{u_2} , have a tendency to be less than 3.0 with values between 2.85 and 3.0. This shows that large-amplitude fluctuations are less probable than expected for a normal distribution. Nevertheless, when only the symmetry of the velocity fluctuation distribution and its form are considered to be the criteria of homogeneity, measured skewness and flatness values downstream of the grid give an impression that the turbulence field is homogeneous although there exists a spatial inhomogeneity of the measured turbulence quantities.

Strained Turbulence

The effect of mean velocity distortion on the homogeneity of the grid-generated turbulence becomes crucial when the dependence of the Reynolds stresses measured along the

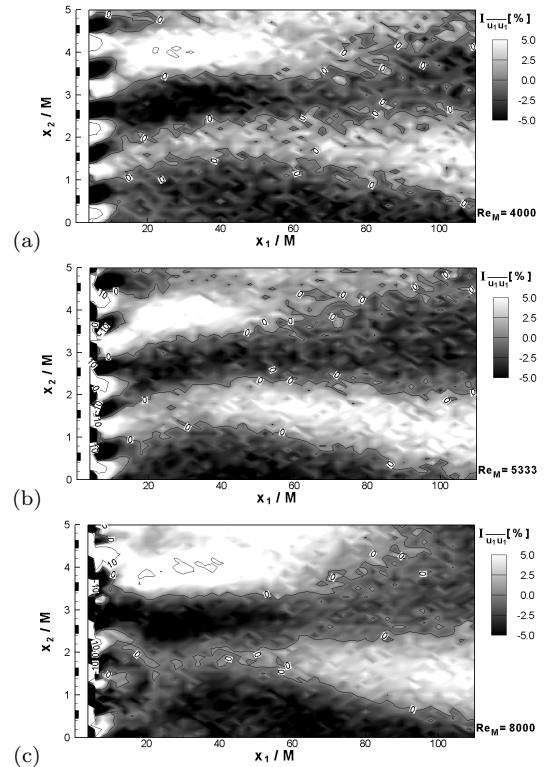


Figure 4: $I_{\overline{u_1 u_1}}$ field at the wake of the grid in the wind tunnel at different mesh Reynolds numbers: $Re_M =$ (a) 4000, (b) 5333 and (c) 8000.

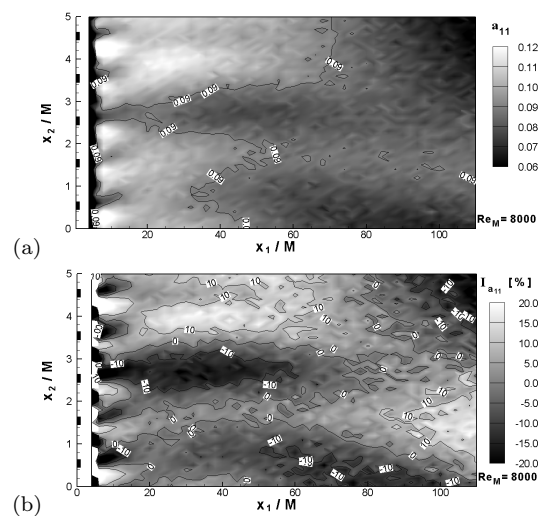


Figure 5: (a) a_{11} field and (b) its inhomogeneity field $I_{a_{11}}$ at the wake of the grid in the wind tunnel at $Re_M = 8000$.

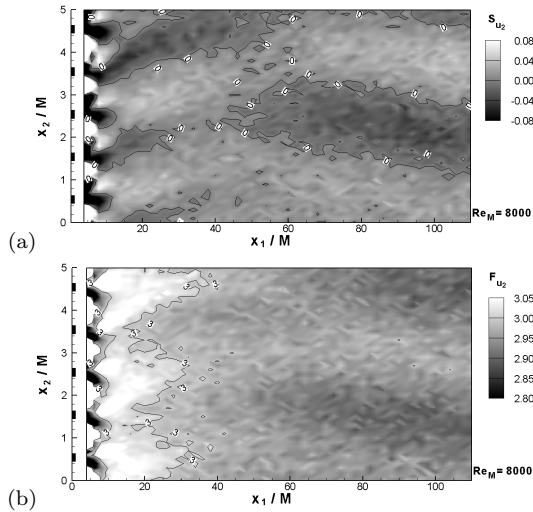


Figure 6: (a) Skewness and (b) flatness factors of u_2 fluctuations at the wake of the grid in the wind tunnel at $Re_M = 8000$.

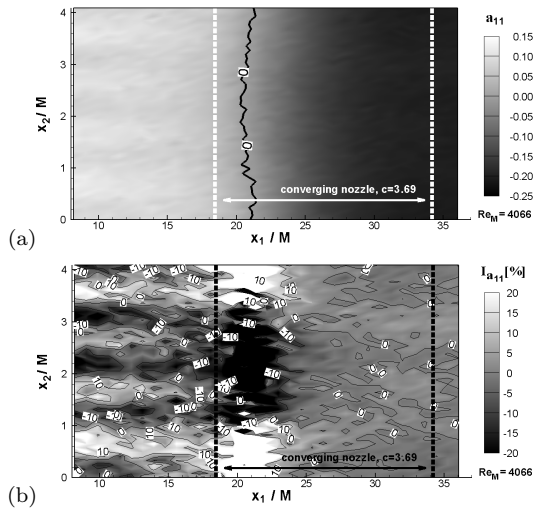


Figure 7: (a) a_{11} field and (b) its inhomogeneity field $I_{a_{11}}$ in the wake of the grid in the AST through the converging nozzle with $c = 3.69$ at $Re_M = 4066$.

symmetry axis of the nozzle relative to the orientation of the grid structure is considered. In the present study, the most remarkable effect of contraction was observed on the inhomogeneity of a_{11} , when inhomogeneous grid-generated turbulence was contracted through the nozzle with $c = 3.69$ as shown in Fig. 7. While turbulence approaches an isotropic state ($a_{11} \rightarrow 0$ in Fig. 7 a), $I_{a_{11}}$ increases, and, after passing this state, $I_{a_{11}}$ decreases to a range $\pm 5\%$ as shown in Fig. 7 b. Interestingly, the isotropic states reached in the contraction seem to function like a barrier, after which the inhomogeneity of the Reynolds stresses drop drastically. It is probable that the mixing effect of turbulence increased with improved isotropy and, consequently, the inhomogeneous turbulence field homogenized.

Influence of Inhomogeneity on the Decay Law Constants

As measurements along one $x_2 = \text{constant}$ line were often used to test homogeneous turbulence models, the kind of spatial inhomogeneity presented here becomes very crucial.

In order to demonstrate this, we considered the constants in the decay laws of various turbulence quantities in grid-generated turbulence. The following forms of power decay law [see, for example, Hinze (1975), pp. 259-277, or Mohamed and Larue (1990)] are commonly used in order to describe the decaying Reynolds stresses, turbulence energy and dissipation rate:

$$\frac{\overline{uu}}{\overline{U}^2} = A_{\overline{uu}} \left(\frac{x}{M}\right)^{n_{\overline{uu}}}, \quad (6a)$$

$$\frac{\overline{vv}}{\overline{U}^2} = A_{\overline{vv}} \left(\frac{x}{M}\right)^{n_{\overline{vv}}}, \quad (6b)$$

$$\frac{\overline{q^2}}{\overline{U}^2} = A_{q^2} \left(\frac{x}{M}\right)^{n_{q^2}}, \quad (6c)$$

$$\frac{\epsilon}{\overline{U}^3} M = A_\epsilon \left(\frac{x}{M}\right)^{n_\epsilon}, \quad (6d)$$

where A_s and n_s are constants of the power decay laws. The value of $n_{\overline{uu}}$ found in the literature varies between 1.0 and 1.43 (Mohamed and Larue, 1990), which is a deviation of almost 40%. The $Re_M = 4000$ case in the wind tunnel and the homogeneity measurement downstream of the nozzle having $c = 1.27$ and conducted at $Re_M = 4066$ (i.e. after straining) are compared in Fig. 8. The comparison is made between their inhomogeneity in q^2 and the constants of decay laws evaluated from least-square curve-fits of the data along $x_2 = \text{constant}$ lines. The nozzle with $c = 1.27$ could reduce a_{11} from 0.09 to 0.03 (Ertuğ, 2007). The inhomogeneity fields I_{q^2} are shown in Fig. 8 a and d for unstrained and strained cases, respectively. As can be seen in these figures, the I_{q^2} field after the contraction is more homogeneous than the unstrained field.

The effect of inhomogeneity on the decay constants is clearly demonstrated in Fig. 8 a, c, e and f. For instance, $A_{\overline{uu}} n_{\overline{uu}}$ can vary by $\pm 55\%$ and $\pm 7\%$, respectively, along the transverse x_2 -axis in a grid-generated turbulence field. Since the inhomogeneity for the turbulence with improved isotropy is less than the simple grid-generated turbulence, the scatter of decay constants of the former along the x_2 -axis is also less (Fig. 8e and f).

CONCLUSIONS

The present investigations on grid-generated turbulence, which were conducted in two different flow facilities, showed that the inhomogeneity of mean velocities decreases rapidly behind the grid, whereas the inhomogeneity of Reynolds stresses persists much longer. Reynolds stresses showed inhomogeneous fields which are composed of elongated positive and negative regions far downstream of the grid. These regions also coalesce with each other. Measurements which were performed in the mesh Reynolds number range 4000 - 8000 did not reveal any dependence of inhomogeneity on the mesh Reynolds number. Interestingly, the inhomogeneous regions remained almost at the same locations but can not be attributed to geometrical tolerances of the grid.

The present findings on the inhomogeneity of decaying grid-generated turbulence are in accordance with those of Grant and Nisbet (1957) and show the dependence of measured mean quantities on the relative position of the measurement location with respect to the grid. The presented results demonstrate that obeying all commonly accepted rules suggested by Corrsin (1963), which were followed in the past by many researchers, does not warrant the generation of a homogeneous turbulent field downstream of static grids.

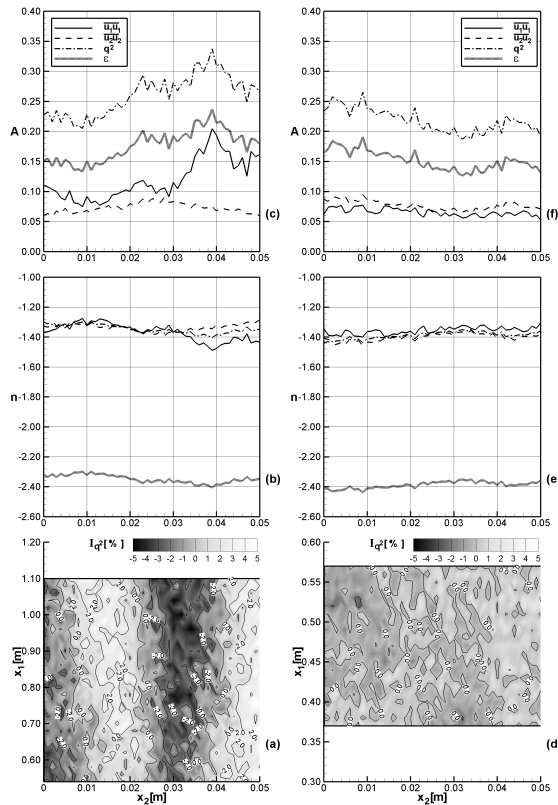


Figure 8: Inhomogeneity field of turbulent energy I_{q2} and the decay law constants, (a), (b) and (c) for unstrained grid-generated turbulence at $Re_M = 4000$ and (d), (e) and (f) for strained grid-generated turbulence downstream of the nozzle with $c = 1.27$ at $Re_M = 4066$.

It is shown that decreasing the anisotropy of grid-generated turbulence by straining it through a nozzle enhances the homogeneity of turbulence. The experiments downstream of the nozzle with $c = 1.27$ showed that the scatter in the decay constants of turbulence drops remarkably. Comte-Bellot and Corrsin (1966) used such a nozzle to improve the isotropy and consequently obtained universal decay constants for isotropic turbulence. It is now clear that they not only reduced the anisotropy but also enhanced the homogeneity of their turbulence and, as a result, they obtained less scatter in the decay constants in their experiments ($1.16 \leq n \leq 1.37$). Any kind of study which does not take inhomogeneity of grid-generated turbulence into consideration can be misleading. Therefore, the authors are of the opinion that this inhomogeneous state of the grid-generated turbulence is probably one of the most important reasons for the discrepancies observed in the decay constants evaluated from the measurements of decaying grid-generated turbulence found in literature.

In addition to the reduction in the anisotropy of turbulence, it is our expectation that increased mixing action of the turbulence generator may enhance the homogeneity of the Reynolds stresses. Increased mixing action can be achieved, for example, by an active grid (Mydlarski and Warhaft, 1996). Nevertheless, the available homogeneity measurements downstream of such active grids are rather scarce.

ACKNOWLEDGMENTS

The authors gratefully acknowledge the scholarships pro-

vided to Özgür Ertunç by the Scientific and Technological Research Council of Turkey and the Bavarian Research Foundation for his PhD studies at FAU LSTM-Erlangen. Without the financial support of LSTM-Erlangen and the Volkswagen Foundation for the construction of the experimental facilities, this study would not have been possible. We would like to thank Prof. Dr. Hassan M. Nagib for providing us with the results of his research on turbulence manipulators.

REFERENCES

Batchelor, G. K. and Stewart, R. W., 1950, "Anisotropy of the Spectrum of Turbulence at Small Wave Numbers", *Q. J. Appl. Math.*, vol. 3, p. 1.

Batchelor, G. K. and Townsend, A. A., 1948, "Decay of Isotropic Turbulence in the Initial Period", *Proc. Roy. Soc. A*, vol. 193, pp. 539-558.

Comte-Bellot, G. and Corrsin, S., 1966, "The use of a contraction to improve the isotropy of grid generated turbulence", *J. Fluid Mech.*, vol. 25, p. 657.

Corrsin, S., 1963, *Turbulence: Experimental Methods*, in Encyclopedia of Physics, vol. 8, Springer, Berlin.

Ertunç, Ö., 2007, *Experimental and Numerical Investigations of Axisymmetric Turbulence*, Ph.D. thesis, Friedrich Alexander Universität Erlangen-Nürnberg, LSTM-Erlangen, URL <http://www.opus.ub.uni-erlangen.de/opus/volltexte/2007/537/>.

Ertunç, Ö. and Durst, F., 2008, "On the high contraction ratio anomaly of axisymmetric contraction of grid-generated turbulence", *Phys. Fluids*, vol. 20, p. 025103.

Ertunç, Ö. and Lienhart, H., 2006, "Inhomogeneity of Grid-Generated Turbulence under Zero Strain and Finite Strain", *Tech. Rep. 697/E*, LSTM-Erlangen.

Ertunç, Ö., Özyılmaz, N., Lienhart, H., Durst, F. and Beronov, K., 2008, "Homogeneity of turbulence generated by static-grid structures", *under consideration in J. Fluid Mech.*

Gence, J. N., 1983, "Homogeneous turbulence", *Annu. Rev. Fluid Mech.*, vol. 15, pp. 201-222.

Grant, H. L. and Nisbet, I. C. T., 1957, "The inhomogeneity of grid turbulence", *J. Fluid Mech.*, vol. 2, pp. 263-272.

Hinze, J. O., 1975, *Turbulence*, 2nd edn., McGraw-Hill, New York.

Liu, R., Ting, D. S.-K. and Rankin, G. W., 2004, "On the generation of turbulence with a perforated plate", *Exp. Thermal and Fluid Sci.*, vol. 28, pp. 307-316.

Loehrke, R. I. and Nagib, H., 1972, "Experiments on Management of Free Stream Turbulence", *Tech. Rep. 598*, AGARD.

Mohamed, M. S. and Larue, J. C., 1990, "The decay power law in grid-generated turbulence", *J. Fluid Mech.*, vol. 219, pp. 195-214.

Mydlarski, L. and Warhaft, Z., 1996, "On the onset of high Reynolds number grid-generated wind tunnel turbulence", *J. Fluid Mech.*, vol. 320, pp. 331-368.